single-molecule fluorescence resonance energy transfer

(4) calculation of κ^2

michael börsch

08/07/2004

fluorescence resonance energy transfer : FRET

distance dependence on nanometer scale: 1-10

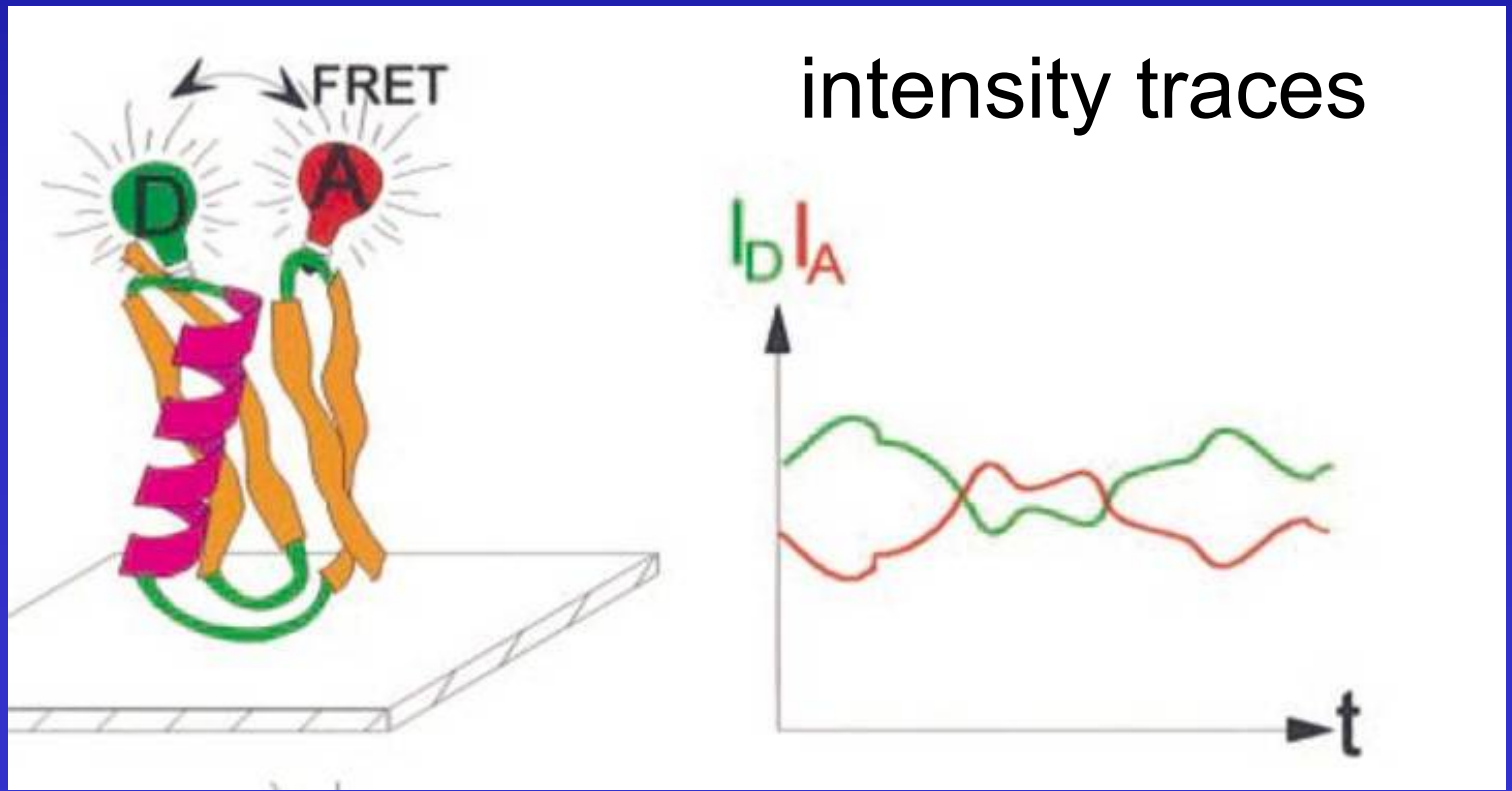

single-molecule FRET: ε-subunit rotation in F_0F_1-ATP synthase

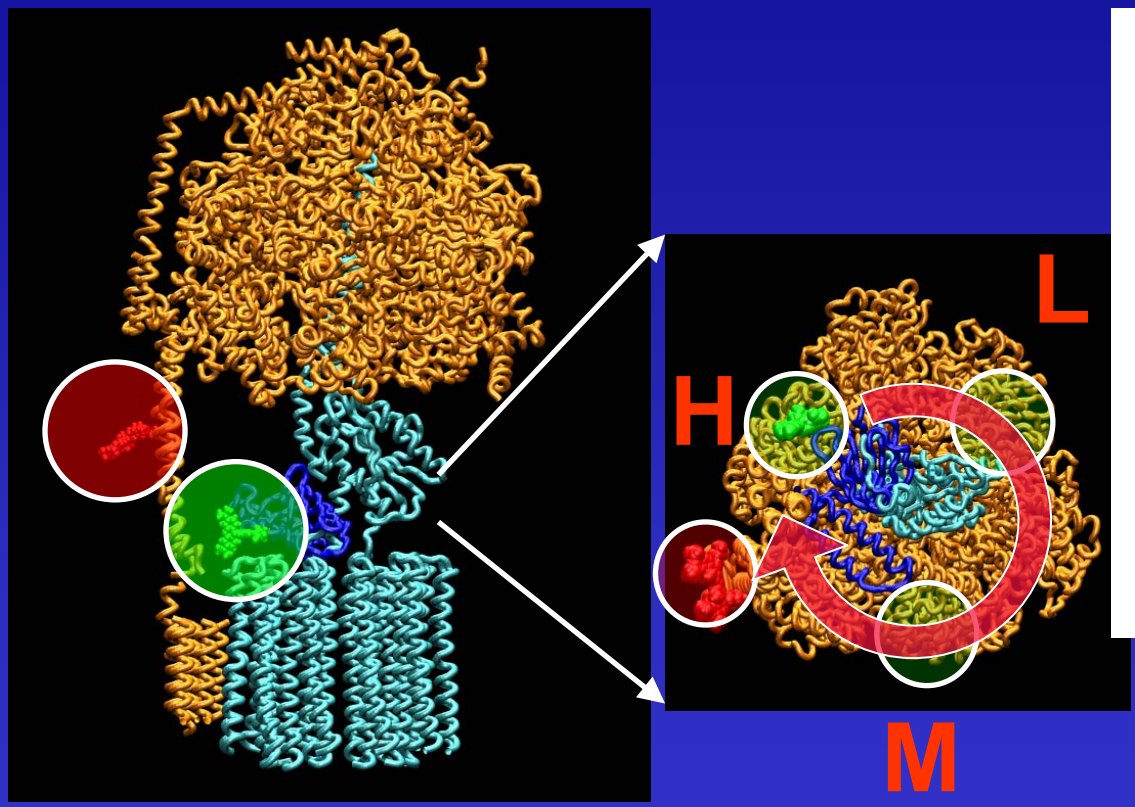

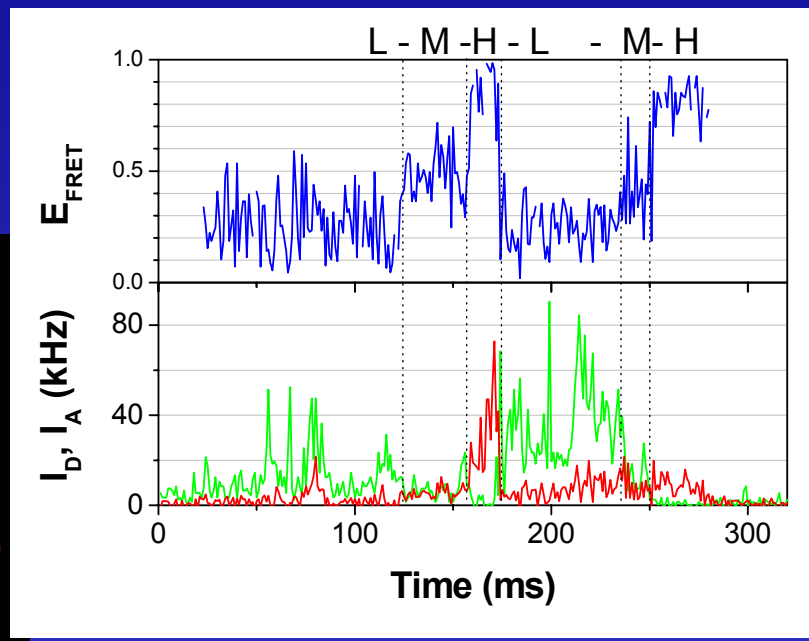

stepwise rotation during ATP synthesis,
B. Zimmermann *et al.*

FRET donor tetramethylrhodamine @ ε (rotating)
FRET acceptor cyanine-5 @ b (static)

→ detecting rotation by cyclic distance changes

Förster theory

- the Förster equation for the RET rate

$$k_T = \frac{9000(\ln 10)\kappa^2 \varphi_D}{128\pi^5 n^4 N_A \tau_D R^6} J$$

- with the spectral overlap integral J, donor quantum yield φ_D , lifetime τ_D
- correlation of FRET efficiency with FRET donor-acceptor distance r

$$E_{FRET} = \frac{R_0^6}{R_0^6 + r^6}$$

- the Förster distance is the distance at which k_T equals $1/\tau_D$

$$R_0^6 = \frac{9000(\ln 10)\kappa^2 \varphi_D}{128\pi^5 n^4 N_A} J$$

→ measure κ^2 for exact distance calculations !

the orientation factor κ^2 (1)

long-range dipole-dipole interaction
→ distance dependent
→ orientation dependent

three orientations:
1. emission transition dipole moment of the donor (*D*-direction)
2. conneting line of the centers of donor and acceptor (*R*-direction)
3. absorption transition dipole moment of the acceptor (*A*-direction)

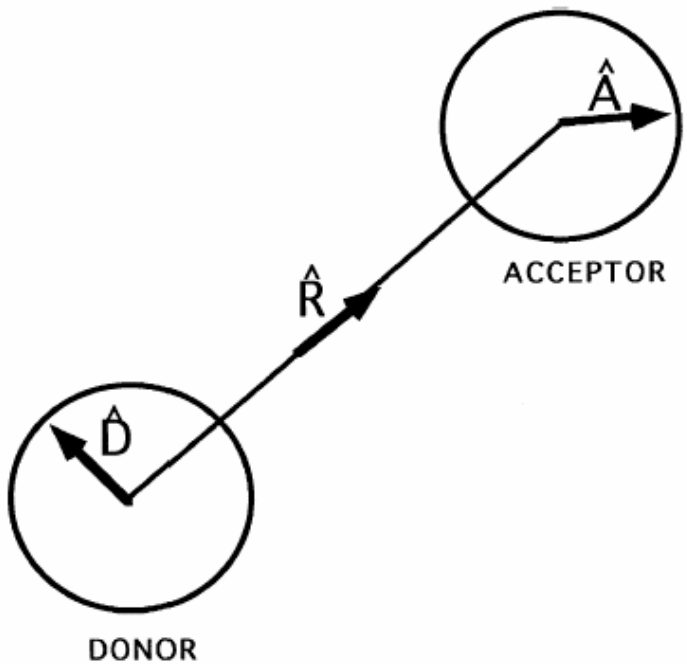

Fig. 1. The unit vectors $\hat{D}$, $\hat{A}$ and $\hat{R}$ are along the D-, A- and R-directions, respectively. $\hat{D}$ is along the emission transition moment of the donor, $\hat{A}$ is along the absorption transition moment of the acceptor, and $\hat{R}$ is along the line from the center of the donor fluorophore to that of the acceptor chromophore. $\hat{D}$, $\hat{A}$ and $\hat{R}$ can lie in one plane, but are in general not co-planar.

the orientation factor κ^2 (2)

- three ways of angular representations:
- θ_D , θ_A ,
- θ_T , φ (*AD*-plane and *AR* plane)
- E_D: oszillating electric field caused by the donor dipole, ω (E_D and *A*)

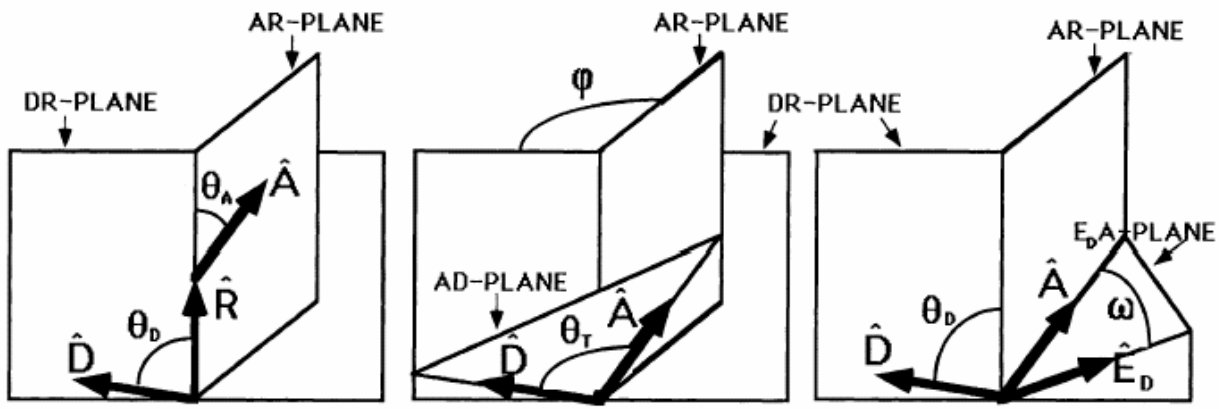

Fig. 2. The polar angles θ_D, θ_A, θ_T and ω, and the azimuthal angle φ:θ_D is between $\hat{D}$ and $\hat{R}$, θ_A is between $\hat{A}$ and $\hat{R}$, θ_T is between $\hat{D}$ and $\hat{A}$, ω is between $\hat{A}$ and the electric field associated with the donor emission moment, and φ is between the projections of $\hat{D}$ and $\hat{A}$ on a plane perpendicular to $\hat{R}$. $\hat{E}_D = (3\hat{R}\cos\theta_D - \hat{D})/\sqrt{1+3\cos^2\theta_D}$ is a unit vector along the electric field associated with the donor emission moment (see Fig. 3). The *DR*-plane is the plane through $\hat{D}$ and $\hat{R}$, the *AR*-plane through $\hat{A}$ and $\hat{R}$, the *DA*-plane through $\hat{D}$ and $\hat{A}$, and the $E_D A$-plane through $\hat{E}_D$ and $\hat{A}$.

the orientation factor κ^2 (3)

3 ways of angular representations

$$\kappa^2 = (\cos\theta_T - 3\cos\theta_D \cos\theta_A)^2$$

$$\kappa^2 = (\sin\theta_D \sin\theta_A \cos\varphi - 2\cos\theta_D \cos\theta_A)^2$$

$$\kappa^2 = \cos^2\omega(1+3\cos^2\theta_D)$$

average for ‹cos²› = 1/3
(for ω and for θ)
→ ‹κ²› = 2/3 ,
if *D*, *A* and *R* are random.

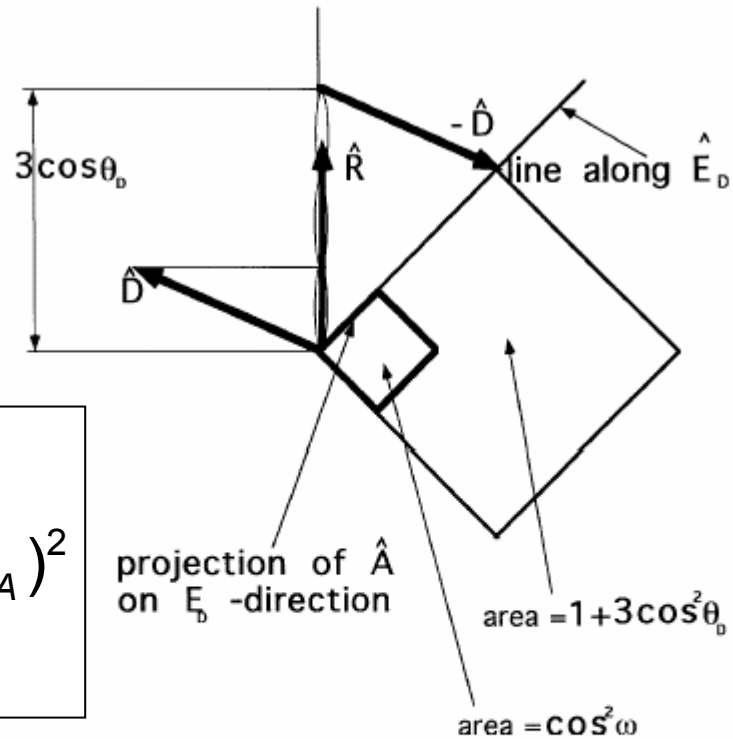

Fig. 3. The relation between the E_D-direction and kappa-squared. The projection of $\hat{D}$ on $\hat{R}$ is $3\cos\theta_D$. The vector sum of $3\hat{R}\cos\theta_D$ and $-\hat{D}$ is along the E_D-direction. The projection of $\hat{A}$ on the E_D-direction is $\cos\omega$. The area of the larger square is $1 + 3\cos^2\theta_D$, that of the smaller square is $\cos^2\omega$. The product of these two areas equals kappa-squared.

the orientation factor κ^2 (4)

- $\kappa^2 = 4$ (transition dipoles antiparallel)
  1 way to be realized

- $\kappa^2 = 0$ (transition dipoles orthogonal)
  infinite number of ways,
  A and E_D are perpendicular

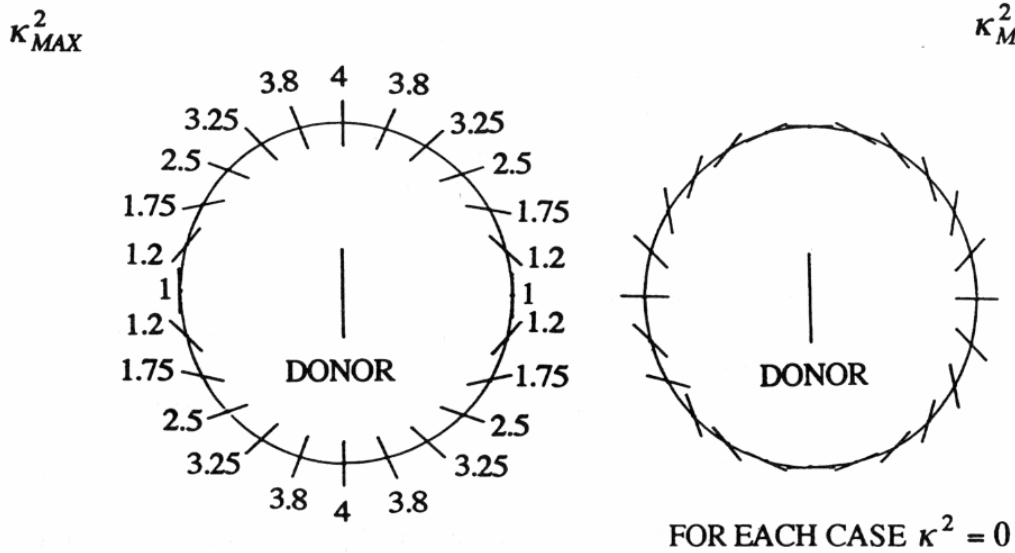

Figure 4.5. Examples of situations in which κ^2 is maximal or minimal. The line segment in the center is along the donor dipole. The line segments on the circles represent possible acceptor dipole orientations. These orientations are such that κ^2 is maximal on the right, and minimal ($\kappa^2 = 0$) on the left. At fixed θ_D, the angle between the donor dipole and the separation vector, there is only one acceptor orientation yielding κ^2_{MAX}, but there is an infinite number of acceptor orientations with $\kappa^2_{MIN} = 0$: orientations perpendicular to the electric dipole field. In the figure only "in-plane" acceptor directions are shown for $\kappa^2_{MIN} = 0$.

- averaging conditions refer to rotational motion during energy transfer time
→ how to measure ?

range of κ^2 values (I)

linear, planar, isotropic polarized

	range	most probable	least probable
L-L	0-4	0	4
L-P	0-2	0.5	2
P-L	0-2	0.5	2
L-I	0.33-1.33	0.33	1.33
I-L	0.33-1.33	0.33	1.33
P-P	0.25-1.25	not known	1.25
P-I	0.33-0.83	0.83	0.33
I-P	0.33-0.83	0.83	0.33
I-I	0.67	0.67 (always)	-

→ most probable values < 1,

→ large deviations from $\kappa^2=2/3$ for L-L case possible

range of κ^2 values (II)

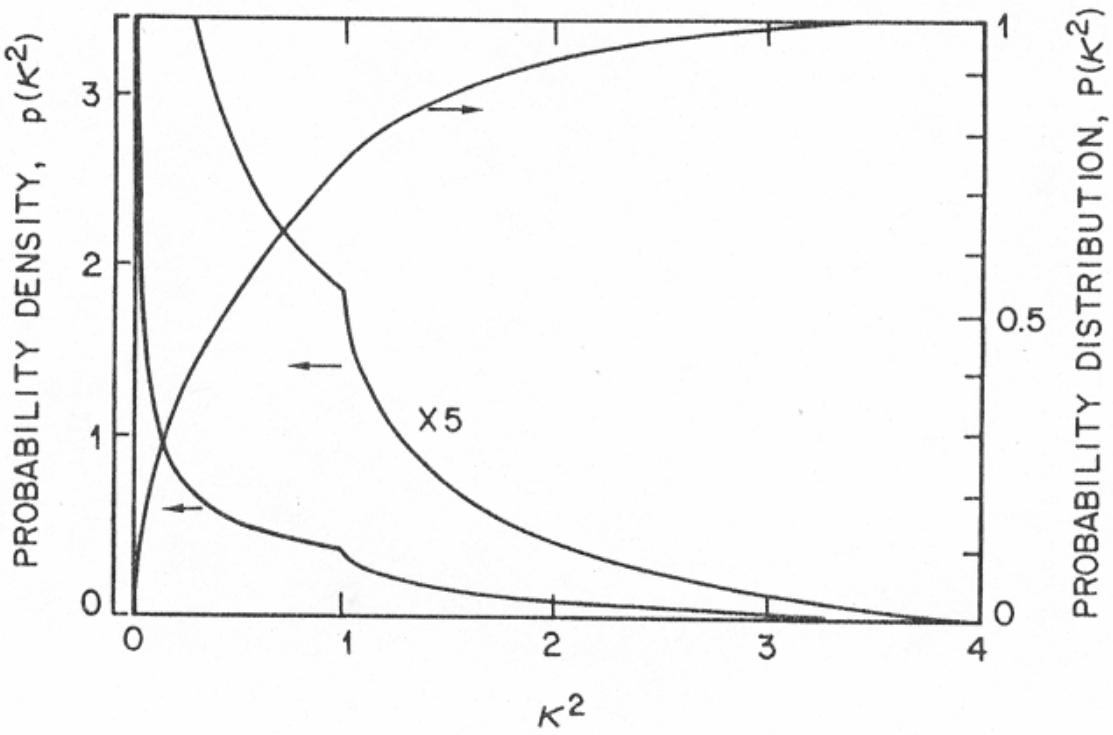

FIGURE 11 The curve $p(\kappa^2)$ gives the probability density that any particular value of κ^2 obtains between two dipoles, each of which may adopt any orientation independently of the other. $P(\kappa^2)$ is the probability distribution of κ^2 having a value between 0 and κ^2. The probability of κ^2 being less than 0.1, for example, is seen to be 0.25.

L-L case

transition dipole moments (I)

polarization [P]

$$P = \frac{I_{\parallel} - I_{\perp}}{I_{\parallel} + I_{\perp}}$$

anisotropy [r]

$$r = \frac{I_{\parallel} - I_{\perp}}{I_{\parallel} + 2I_{\perp}}$$

1. in isotropic solution: EX with linearly polarized light

⇒ selective excitation of absorption dipoles parallel to the electric vector (photoselection).

2. rotational diffusion during fluorescence lifetime

⇒ depolarization

transition dipole moments (II)

angular displacement α between absorption and emission dipole moments

α:	0°	45°	54.7°	90°
r_0:	0.40	0.10	0.00	-0.20
P_0:	0.50	0.14	0.00	-0.33

1. linear polarized
2. planar polarized (naphthyl ?)
3. isotropic polarized or triply-degenerized: lanthanide ions Eu^{3+}

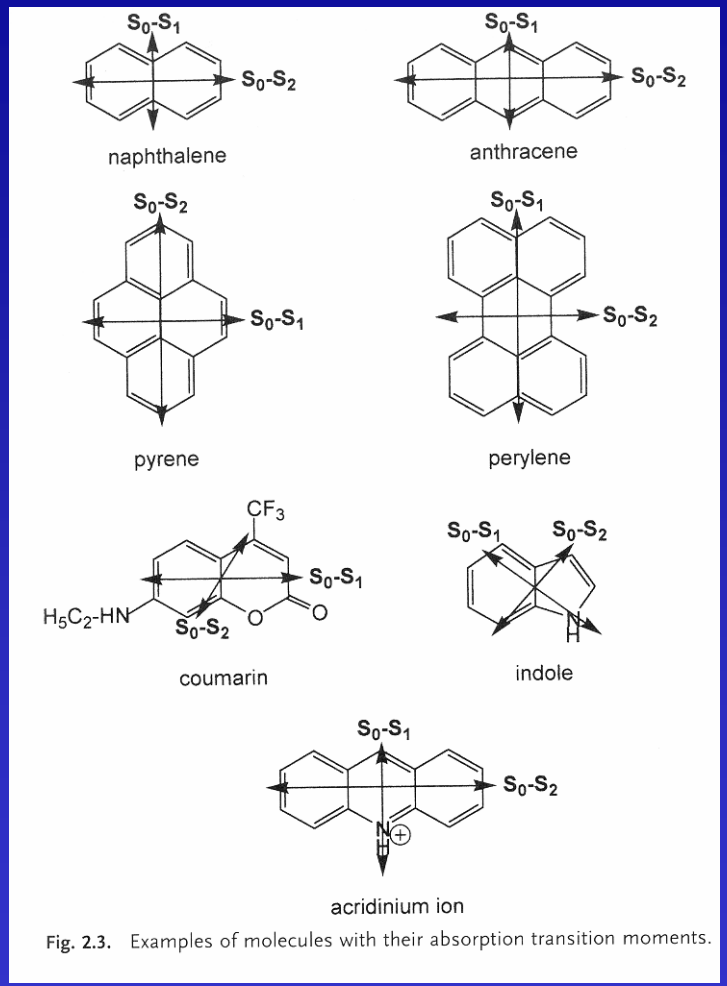

Fig. 2.3. Examples of molecules with their absorption transition moments.

measured in frozen solution, (→ EtOH 95% @ 77K)

time-resolved anisotropy r(t) (I)

$$r = \frac{I_{\parallel} - I_{\perp}}{I_{\parallel} + 2I_{\perp}}$$

$$r(t) = r_0(t=0) \bullet \exp(-t/\phi_{rot})$$

$$I(t)_{\perp,\parallel} = I(t=0)_{\perp,\parallel} \bullet \exp\left(\frac{-t}{\tau_{\perp,\parallel}}\right)$$

with τ : FL lifetime

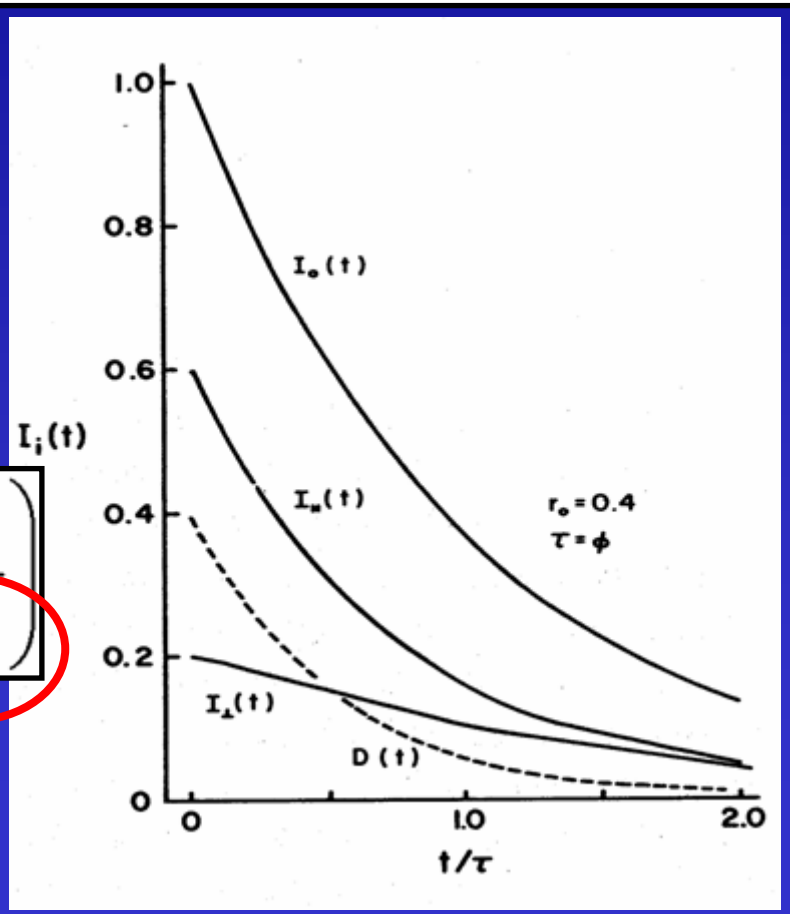

time-resolved anisotropy r(t) (II)

$$r(t) = r_0(t=0) \bullet \exp(-t / \phi_{rot})$$

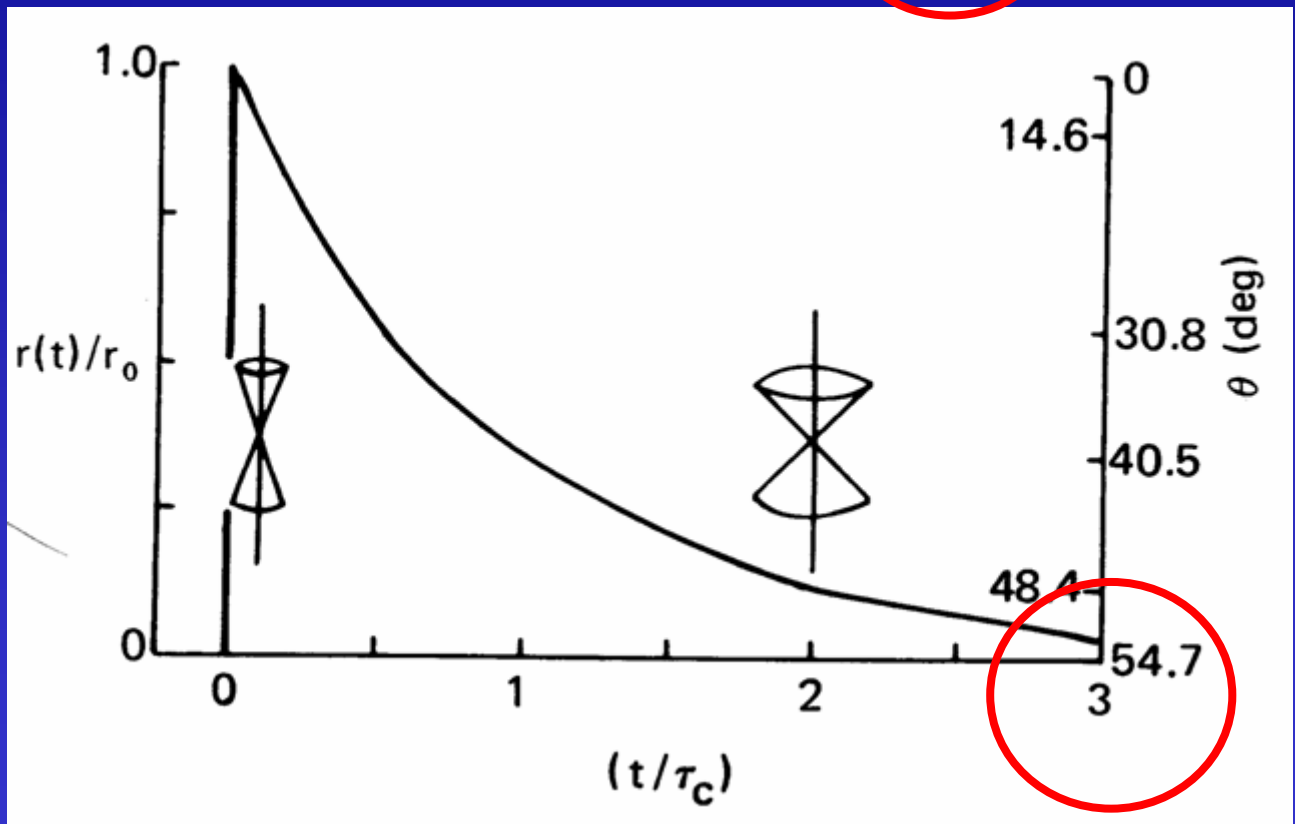

angular displacement between transition dipole moments results in fluorescence depolarization due to rotational diffusion

time-resolved anisotropy (III)

example I:

rhodamine 6 G in glycol

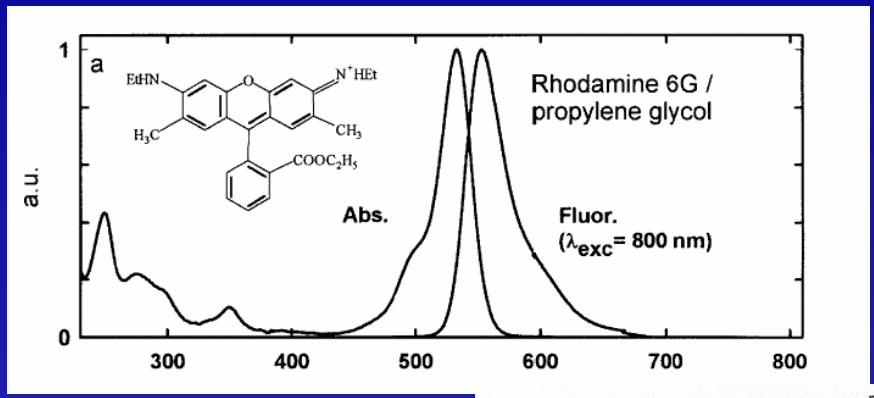

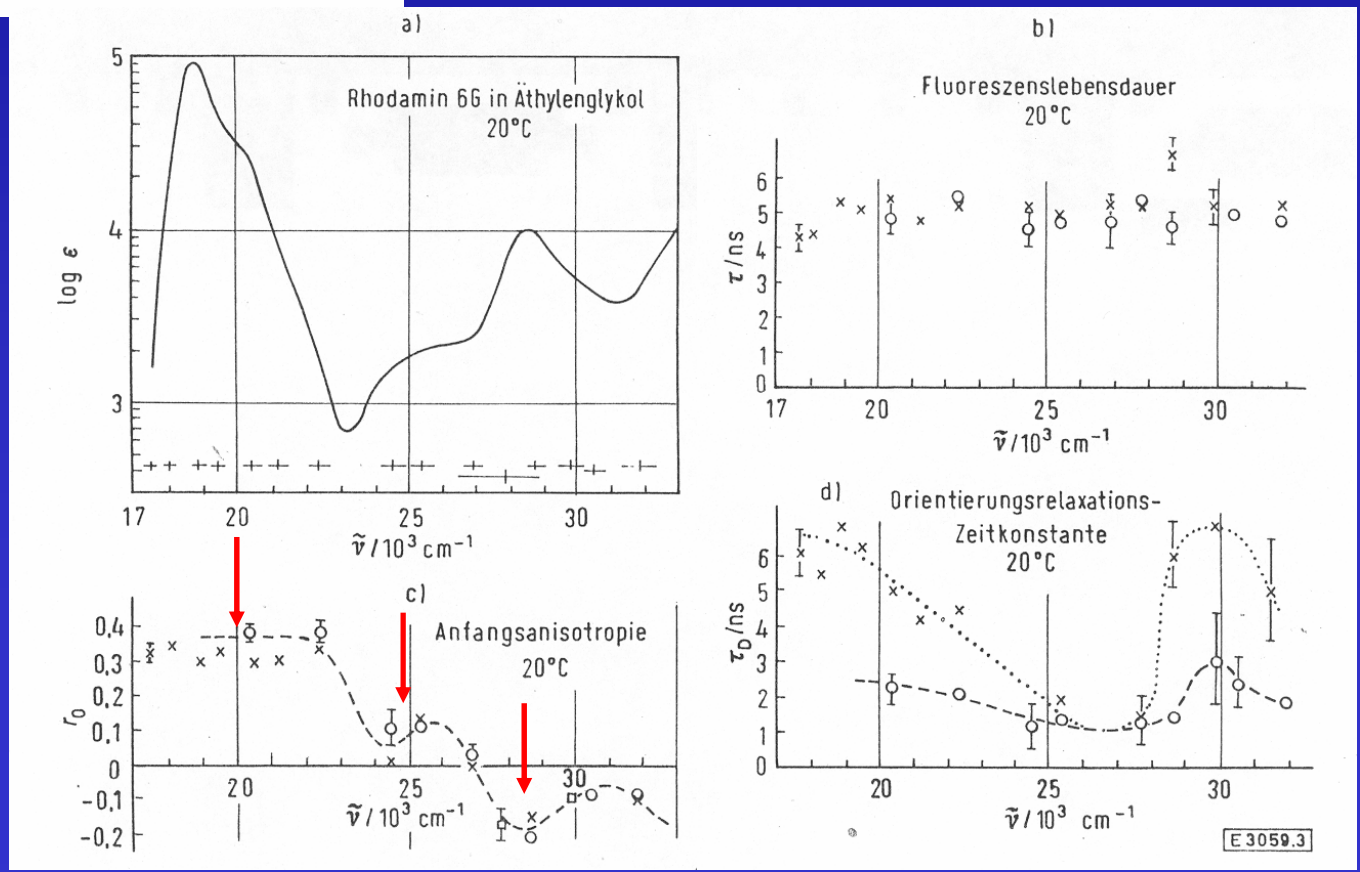

time-resolved anisotropy (IV)

Table 1. Fluorescence intensity and anisotropy decay parameters for DPH and R6G after TPE and for *p*-terphenyl after ThPE in propylene glycol at 300 K compared with OPE.

	Fluorescence decay parameters				Anisotropy decay parameters			
	λ_{exc} nm^{-1}	τ_1, τ_2 ns^{-1}	α_k %	XSQ	τ_r ns^{-1}	r_0	r_∞	XSQ
R 6G	800	3.50 ± 0.02	98.4	1.150	8.19 ± 0.69	0.496 ± 0.011	0.009 ± 0.008	1.055
		0.16 ± 0.06	1.6					
	400	3.51 ± 0.02	98.4	1.318	6.16 ± 1.10	0.088 ± 0.004	0.003 ± 0.003	1.080
		0.19 ± 0.08	1.6					

2-photon-excitation results in higher r_0 values (> 0.4)

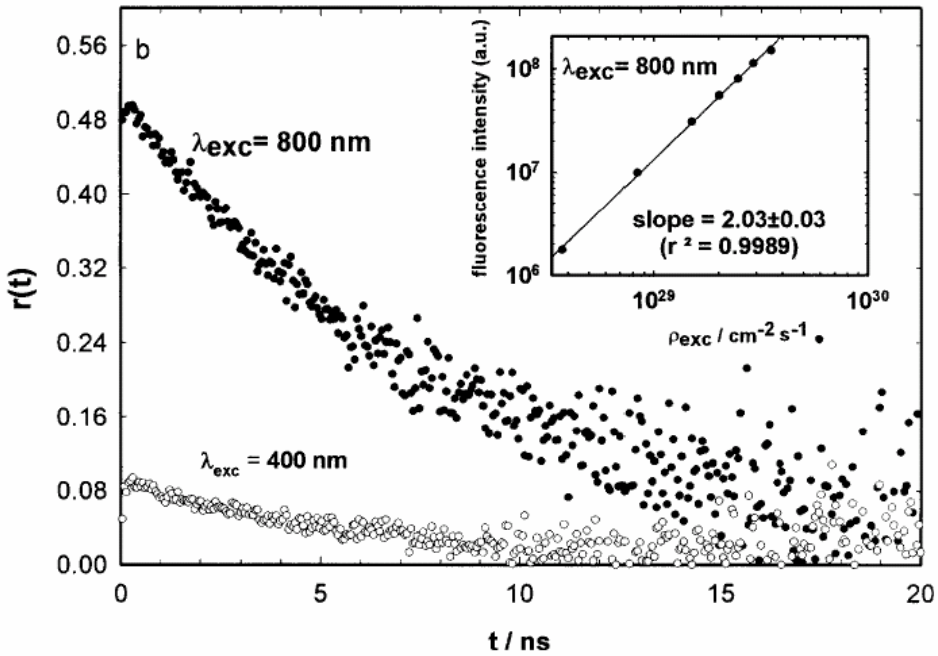

A. Volkmer *et al.*, Meas. Sci. Technol. 8, 1339-1349 (1997)

Figure 7. (a) Fluorescence spectra of 5×10^{-6} M solution of R6G in propylene glycol excited at 800 nm and at 300 K. (The absorption spectrum is also shown.) (b) Fluorescence anisotropy decay measured for one-photon (○: λ_{exc} = 400 nm) and two-photon (●: λ_{exc} = 800 nm) excitation. The log–log plot of R6G fluorescence intensity dependence in propylene glycol on the incident photon flux density at 800 nm is shown in the inset.

rotational diffusion

- fluorophor
- with flexible linker
- bound to amino acid
- of a flexible part of a sub-unit
- conformational changes
- association / dissociation

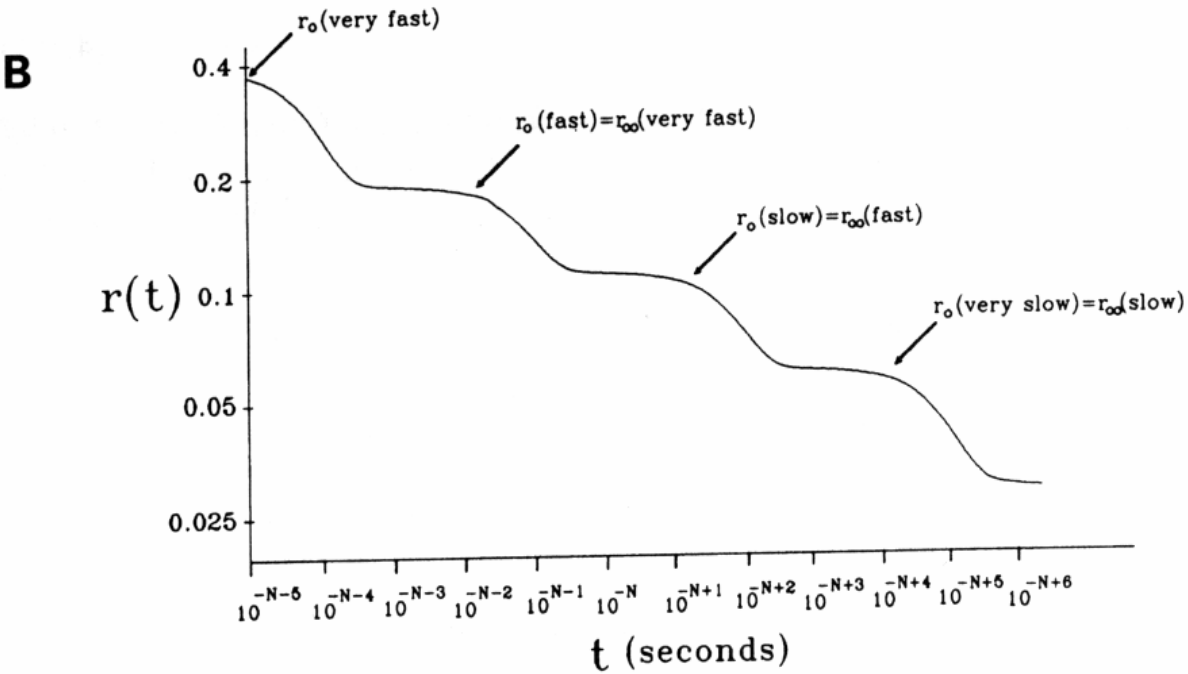

Figure 4.10. The anisotropy $r(t)$ versus the time t for $r(t)$ given by Eq. (4.19) as a linear multiscale plot (A) and as a log–log plot (or Bürkli-Cherry plot [21]) (B), where $r_{01} = r_0$(very fast) = the fundamental anisotropy, $r_{02} = r_0$(fast), $r_{03} = r_0$(slow), and $r_{04} = r_0$(very slow). In A: VSTU = very short time units (e.g., femtoseconds), STU = short time units (e.g., picoseconds) (1 STU = 1000 VSTU), LTU = large time units (e.g., nanoseconds) (1 LTU = 1000 STU), VLTU = very large time units (e.g., microseconds) (1 VLTU = 1000 LTU). In B:N represents any integer. If, for example, N would be equal to 10, the scale would extend from femtoseconds to 0.1 milliseconds. The parameter values are: in A: $r_{01} = 0.39$, $r_{02} = 0.31$, $r_{03} = 0.21$, $r_{04} = 0.12$, $r_{05} = 0.05$, $\varphi_1 = 0.5$ VSTU, $\varphi_2 = 0.5$ STU, $\varphi_3 = 0.5$ LTU, and $\varphi_4 = 0.5$ VLTU; in B: $r_{01} = 0.39$, $r_{02} = 0.19$, $r_{03} = 0.11$, $r_{04} = 0.06$, $r_{05} = 0.03$, and, in seconds: $\varphi_1 = 10^{-N-4}$, $\varphi_2 = 10^{-N-1}$, $\varphi_3 = 10^{-N+2}$, and $\varphi_4 = 10^{-N+5}$.

Soleillet's theorem (1929)

- for a series of depolarizing steps

$$r = 0.4 \bullet \prod_i d_i$$

with d_i represents depolarization factors,

$$d_i = \tfrac{3}{2}\cos^2\theta_i - \tfrac{1}{2} \quad \longrightarrow \quad \langle d_i \rangle = \tfrac{3}{2}\langle \cos^2\theta_i \rangle - \tfrac{1}{2}$$

and θ_i being the angle by which the transition moment is changed in the i^{th} step

the orientation factor κ^2 (4)

FRET:
3 depolarizing steps:
donor, acceptor and transfer depolarization

1. dynamic averaging regime: random reorientation during transfer time
2. static averaging regime for the case when the rates of rotation are slow compared to the transfer time

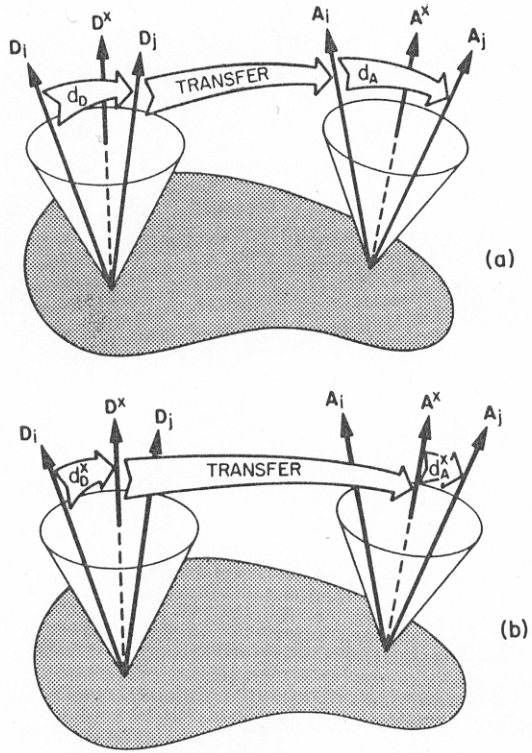

FIGURE 2 (*a*) Schematic representation of the three depolarizing steps after the absorption of excitation energy by the donor: donor depolarization, transfer depolarization, and acceptor depolarization. It is shown in the text that the depolarization corresponding to these steps is the same as in the three depolarizing events shown in *b*: axial depolarization of the donor, depolarization due to transfer between the axes of the orientational distributions of **D** and **A**, and axial depolarization of the acceptor.

the orientation factor κ^2 (5)

Dale et al. (1979)

average transfer depolarization factor:

$$\langle d_T \rangle = \left(\tfrac{3}{2}\langle \cos^2 \psi_D \rangle - \tfrac{1}{2}\right)\left(\tfrac{3}{2}\langle \cos^2 \Theta_T \rangle - \tfrac{1}{2}\right)\left(\tfrac{3}{2}\langle \cos^2 \psi_A \rangle - \tfrac{1}{2}\right)$$

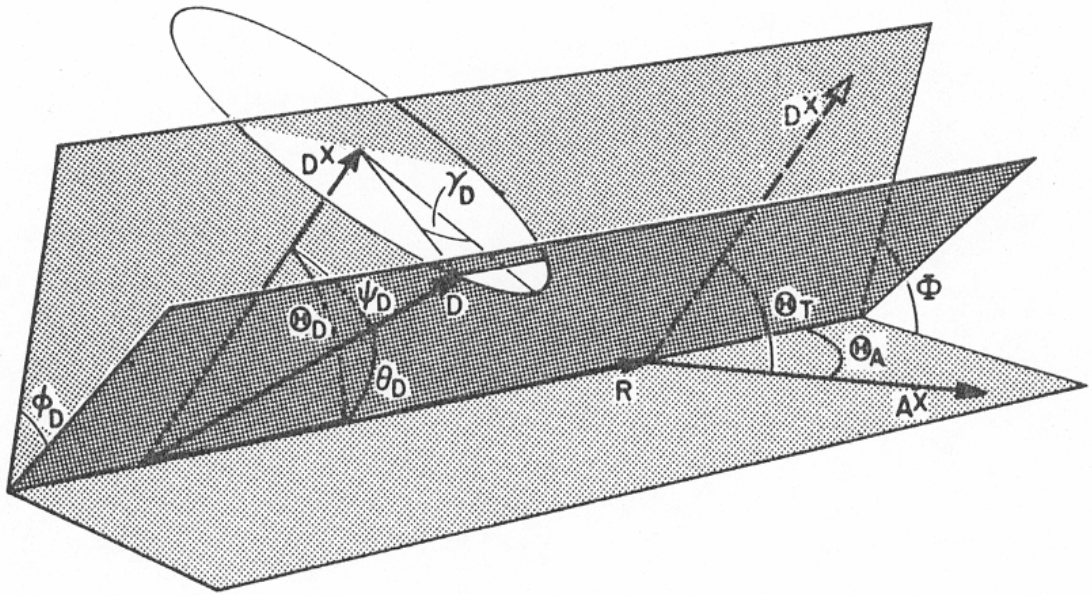

FIGURE 3 Analogous to Fig. 1, except that the place of the D and A transition moments is taken by the symmetry axes (D^x and A^x) of their distributions. This model is used in evaluating the orientation and depolarization factors in terms of the angular parameters ψ_D and γ_D, indicated along with the corresponding acceptor parameters ψ_A and γ_A, omitted here for clarity.

Dale et al. (1979)

the orientation factor κ^2 (6)

... and average value of orientation factor:

$$\left\langle \kappa^2 \right\rangle = \kappa^{x2} \left\langle d_D^x \right\rangle \left\langle d_A^x \right\rangle + \tfrac{1}{3}\left(1-\left\langle d_D^x \right\rangle\right) + \tfrac{1}{3}\left(1-\left\langle d_A^x \right\rangle\right) +$$

$$\cos^2\Theta_D \left\langle d_D^x \right\rangle \left(1-\left\langle d_A^x \right\rangle\right) + \cos^2\Theta_A \left\langle d_A^x \right\rangle \left(1-\left\langle d_D^x \right\rangle\right)$$

$$\text{with} \quad \kappa^{x2} = \left(\sin\Theta_D \sin\Theta_A cos\Phi - 2\cos\Theta_D \cos\Theta_A\right)^2$$

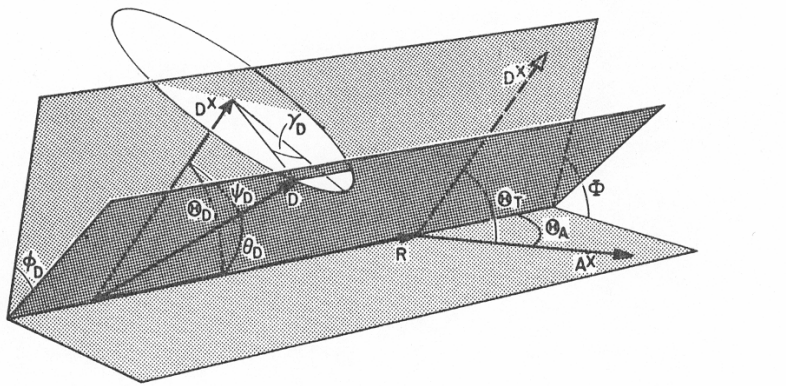

FIGURE 3 Analogous to Fig. 1, except that the place of the D and A transition moments is taken by the symmetry axes (D^x and A^x) of their distributions. This model is used in evaluating the orientation and depolarization factors in terms of the angular parameters ψ_D and γ_D, indicated along with the corresponding acceptor parameters ψ_A and γ_A, omitted here for clarity.

calculating minimum and maximum values of the orientation factor by differentiation

and graphical analysis using in contour plots ...

the orientation factor κ^2 (7)

Dale et al. (1979)

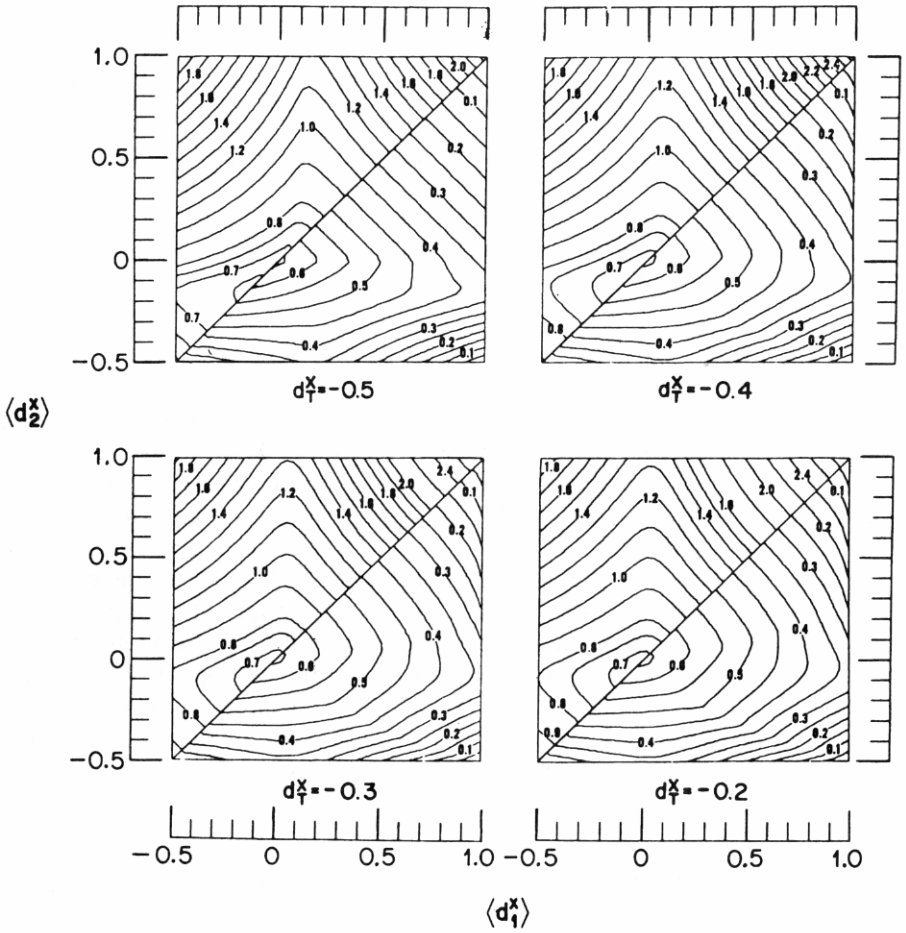

Figure 4.13. Contour plots for obtaining extreme values of $\langle \kappa^2 \rangle$ consistent with the observed donor, acceptor, and transfer depolarization factors, $\langle d_D^X \rangle$, $\langle d_A^X \rangle$, and d_T^X, respectively. Plots are shown for $d_T^X = -0.5, -0.4, -0.3,$ and -0.2. To read the maximum $\langle \kappa^2 \rangle$, take $\langle d_2^X \rangle$ equal to the largest of $\langle d_D^X \rangle$ and $\langle d_A^X \rangle$, and $\langle d_1^X \rangle$ equal to the smallest; to read the minimum, let $\langle d_2^x \rangle$ be the smallest, the $\langle d_1^X \rangle$ be the largest. (Reproduced from the *Biophysical Journal*, 1979, vol. 26, p.170 [3] by copyriht permission of the Biophysical Society.)

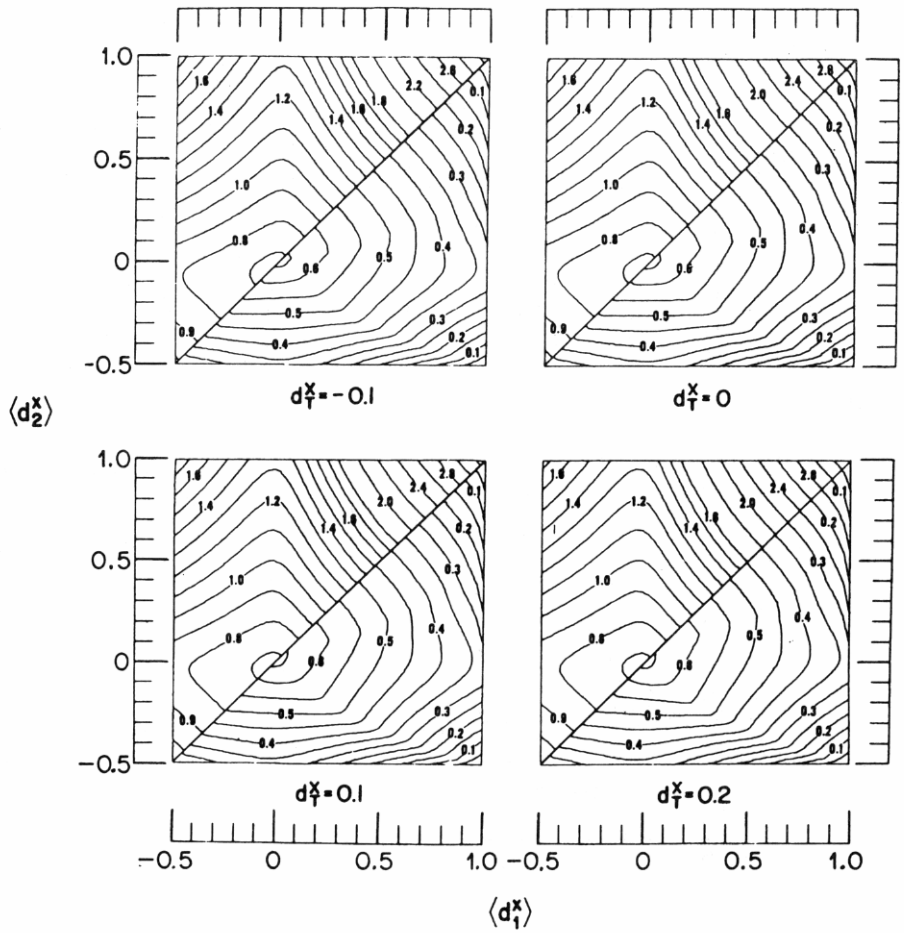

Figure 4.14. Contour plots for obtaining upper and lower limits of $\langle \kappa^2 \rangle$, as in Figure 4.13, but for $d_T^X = -0.1, 0, 0.1,$ and 0.2. (Reproduced from the *Biophysical Journal*, 1979, vol. 26, p.171 [3] by copyright permission of the Biophysical Society.)

the orientation factor κ^2 (8)

Dale et al. (1979)

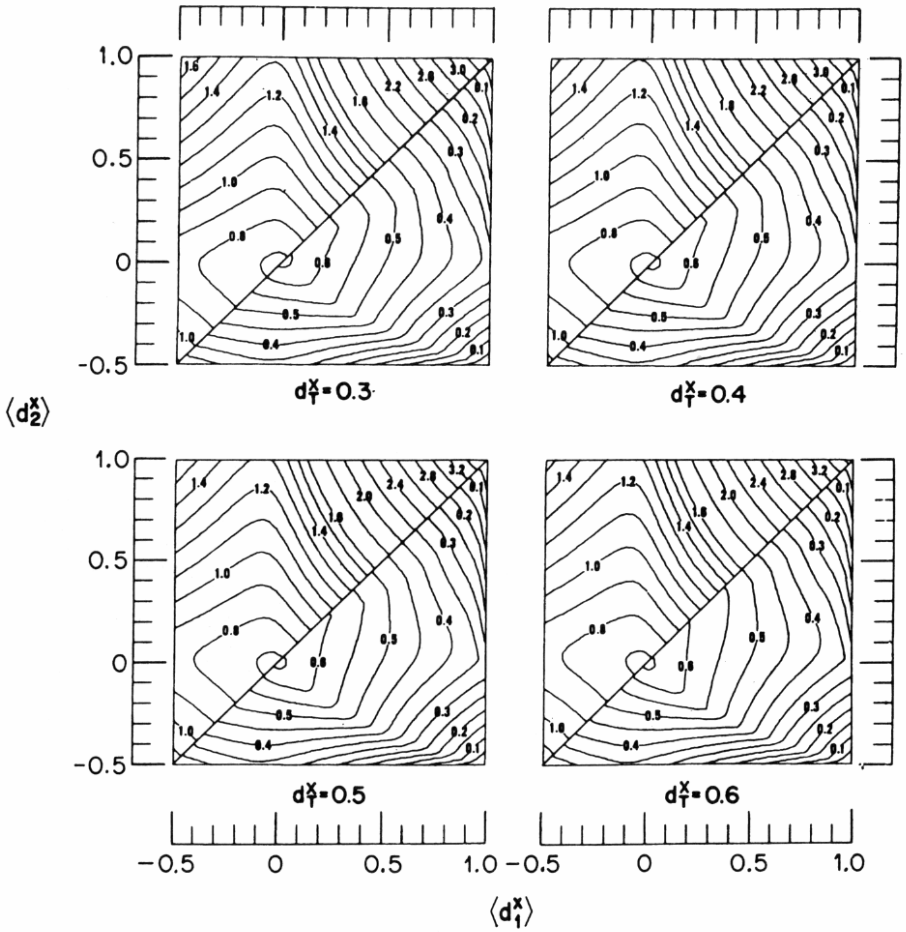

Figure 4.15. Contour plots for obtaining upper and lower limits of $\langle \kappa^2 \rangle$, as in Figure 4.13, but for $d_T^X = 0.3, 0.4, 0.5,$ and 0.6. (Reproduced from the *Biophysical Journal*, 1979, vol. 26, p. 172 [3] by copyright permission of the Biophysical Society.)

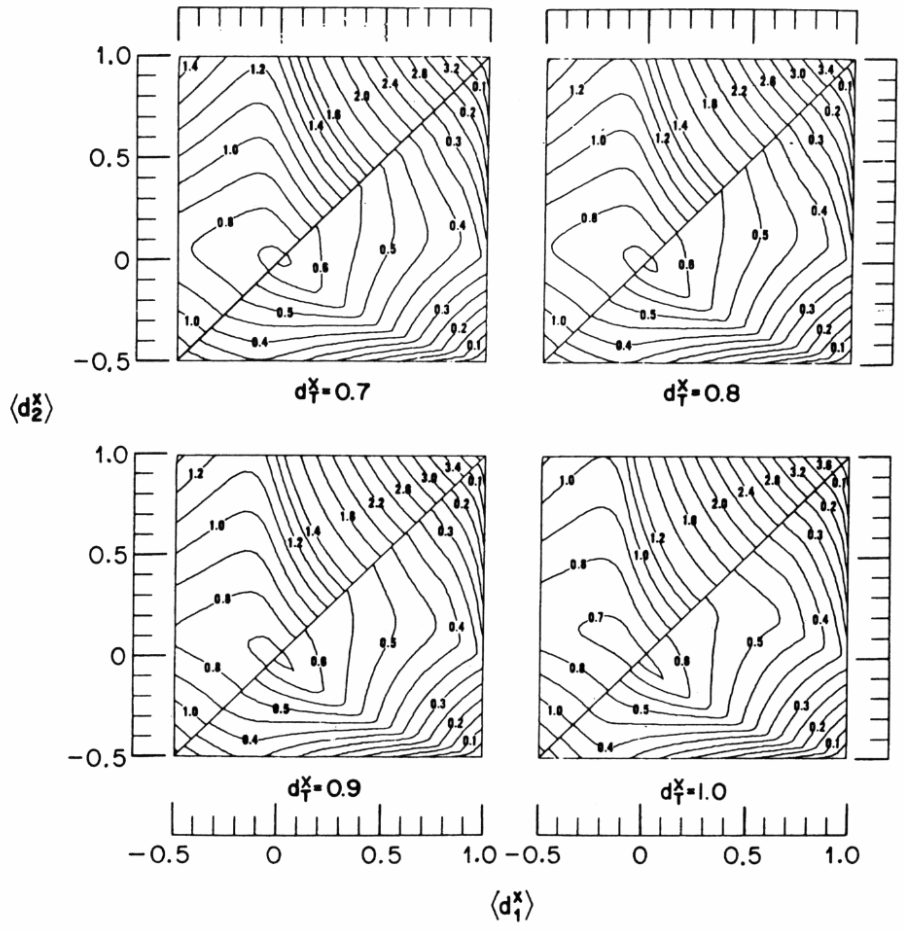

Figure 4.16. Coutour plots for obtaining upper and lower limits of $\langle \kappa^2 \rangle$, as in Figure 4.13, but for $d_T^X = 0.7, 0.8, 0.9,$ and 1.0. (Reproduced from the *Biophysical Journal*, 1979, vol. 26, p. 173 [3] by copyright permission of the Biophysical Society.)

the orientation factor κ^2 (9)

Dale et al. (1979)

- measuring the depolarization factors (values 0 to1):

$$\langle d_D \rangle = \left\langle d_D^x \right\rangle^2 = r_{0D} / 0.4$$

$$\langle d_A \rangle = \left\langle d_A^x \right\rangle^2 = r_{0A} / 0.4$$

- note that ‹d^x› has positive and negative values

- plus independent structural information (i.e. X-ray diffraction)

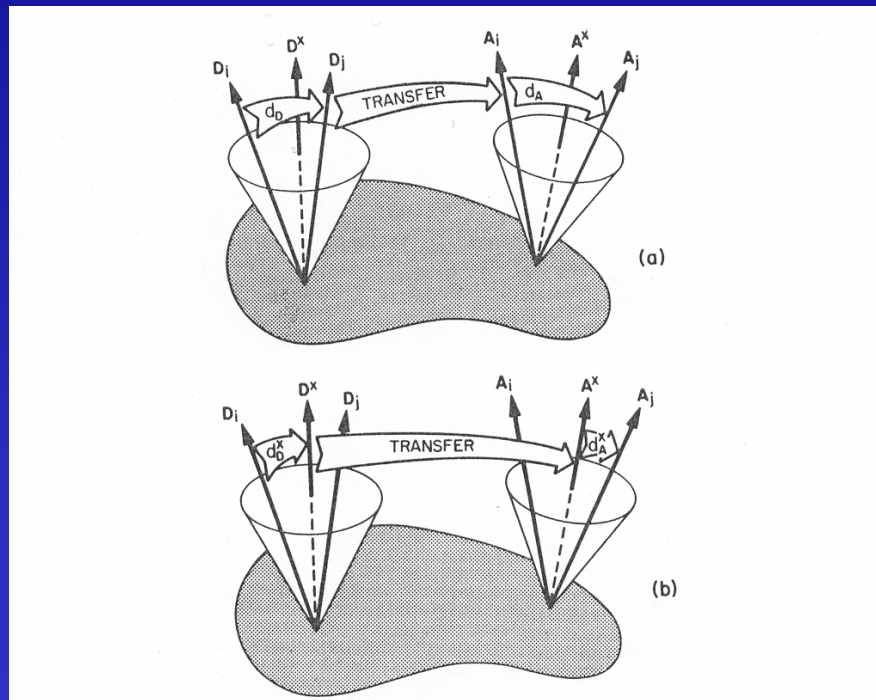

FIGURE 2 (*a*) Schematic representation of the three depolarizing steps after the absorption of excitation energy by the donor: donor depolarization, transfer depolarization, and acceptor depolarization. It is shown in the text that the depolarization corresponding to these steps is the same as in the three depolarizing events shown in *b*: axial depolarization of the donor, depolarization due to transfer between the axes of the orientational distributions of **D** and **A**, and axial depolarization of the acceptor.

the orientation factor κ^2 (10)

Dale et al. (1979)

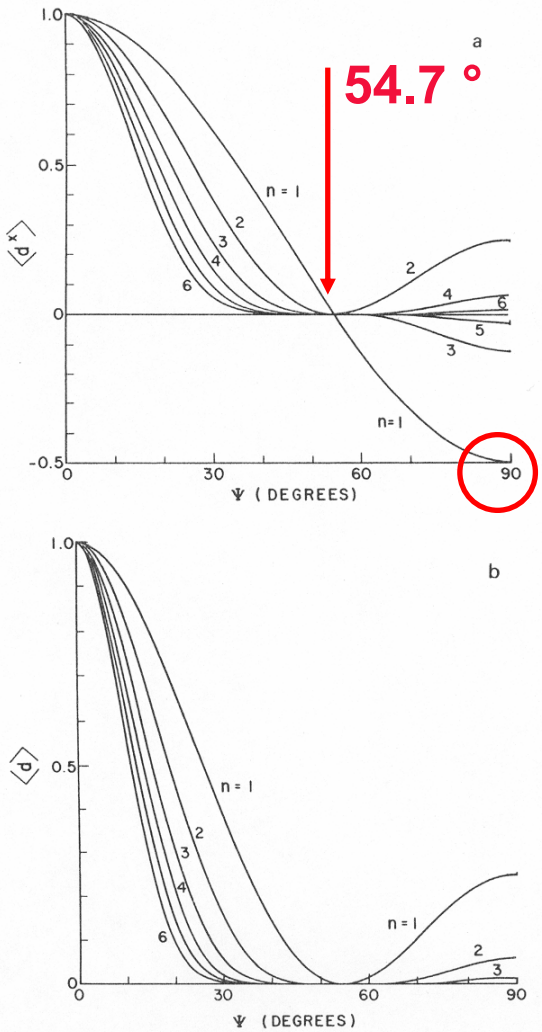

FIGURE 12 The curves labeled $n = 1$ in *a* and *b* give the axial and observed depolarization factors, respectively, for a luminophore constrained to the surface of a cone of half-angle Ψ. This orientational constraint corresponds to the existence of a single, freely rotatable bond between the luminophore and the substrate. The remaining curves, labeled $n = 2, 3, 4, 5, 6$, correspond to n equivalent rotatable bonds between luminophore and substrate and are seen to give rise to ever-decreasing depolarization factors.

the depolarization factor depends on

1. constraints of fluorophore movements in a cone of half-angle Ψ

2. the number of rotatable bonds in the linker between fluorophore and protein

the orientation factor κ^2 (11)

and the error on distance determination by FRET

$$\langle k_T \rangle = \langle \kappa^2 \rangle k_D \, 3/2 \left(\overline{R_0} / R \right)^6$$

1. range probability of κ^2
2. probability distribution for κ^2 : $p(\kappa^2)$
3. relative distance distribution Q(ρ) ≡Q(R)
   ρ=R/R' : ratio of relative distance to R' with κ^2=2/3

$$\kappa^2 = 2/3 \, \rho^6 \quad \Leftrightarrow \quad \rho = \left(3/2 \, \kappa^2 \right)^{1/6}$$

B.W. van der Meer (2002)

the orientation factor κ^2 (12)

and the error on distance

- $p(\kappa^2)$ is always at or near the minimum κ^2

B.W. van der Meer (1994)

Table 4.1 Probabilities of Finding κ^2 Values Within a Given Interval in a Statistically Random Ensemble of Orientations*

Range of κ^2	Probability
$0-\frac{1}{3}$	0.4390
$\frac{1}{3}-\frac{2}{3}$	0.1818
$\frac{2}{3}-1$	0.1395
$1-\frac{4}{3}$	0.0848
$\frac{4}{3}-\frac{5}{3}$	0.0522
$\frac{5}{3}-2$	0.0357
$2-\frac{7}{3}$	0.0250
$\frac{7}{3}-\frac{8}{3}$	0.0174
$\frac{8}{3}-3$	0.0118
$3-\frac{10}{3}$	0.0075
$\frac{10}{3}-\frac{11}{3}$	0.0040
$\frac{11}{3}-4$	0.0012

* Numbers are accurate to the nearest 0.0001.

the orientation factor κ^2 (13)

and the error on distance

- $p(\kappa^2)$ is always at or near the minimum κ^2
- $Q(\rho)$ is shifted towards distances corresponding with higher κ^2

$$\kappa^2 = \tfrac{2}{3}\rho^6 \quad \Leftrightarrow \quad \rho = \left(\tfrac{3}{2}\kappa^2\right)^{1/6}$$

B.W. van der Meer (2002)

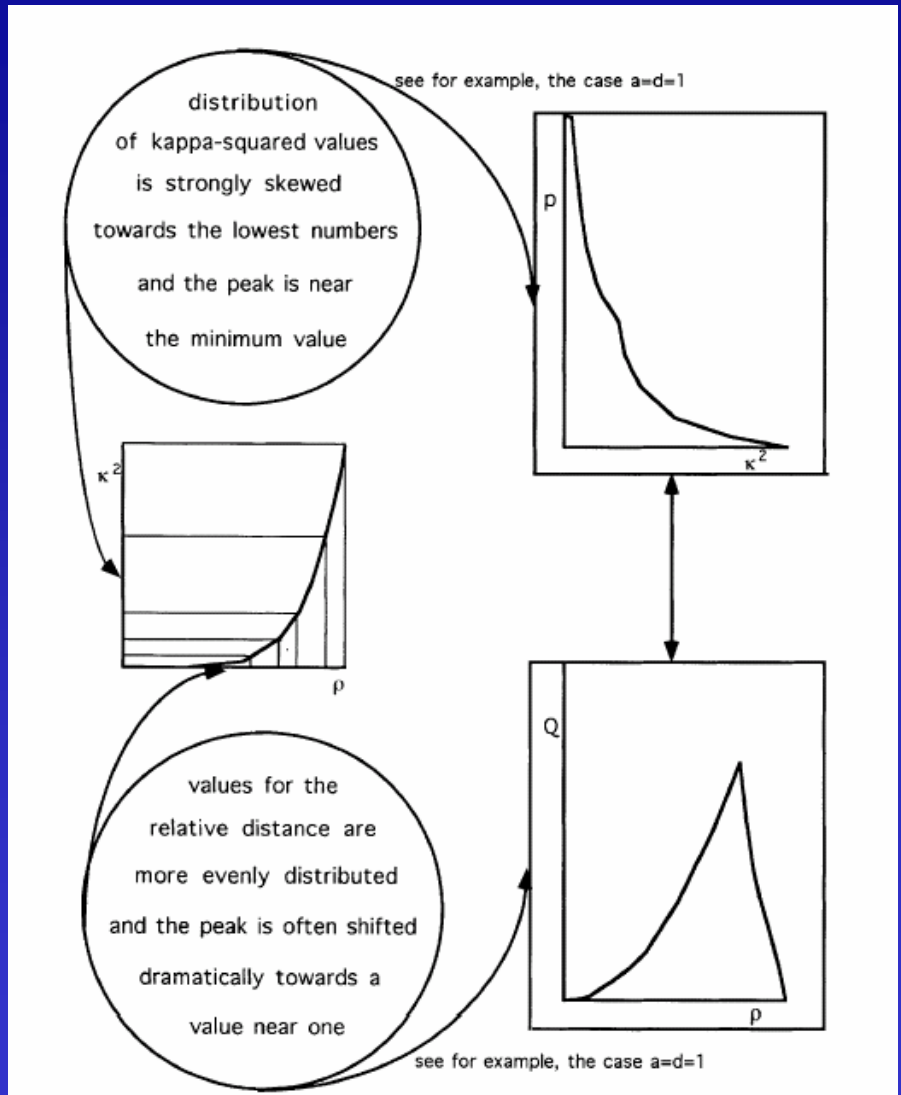

Fig. 4. The effect of $\kappa^2 = \frac{2}{3}\rho^6$ on the relation between $p(K^2)$ and $Q(\rho)$.

the orientation factor κ^2 (14)

and the error on distance determination by FRET

fixed transition dipole moments | partly free | one fixed + one free

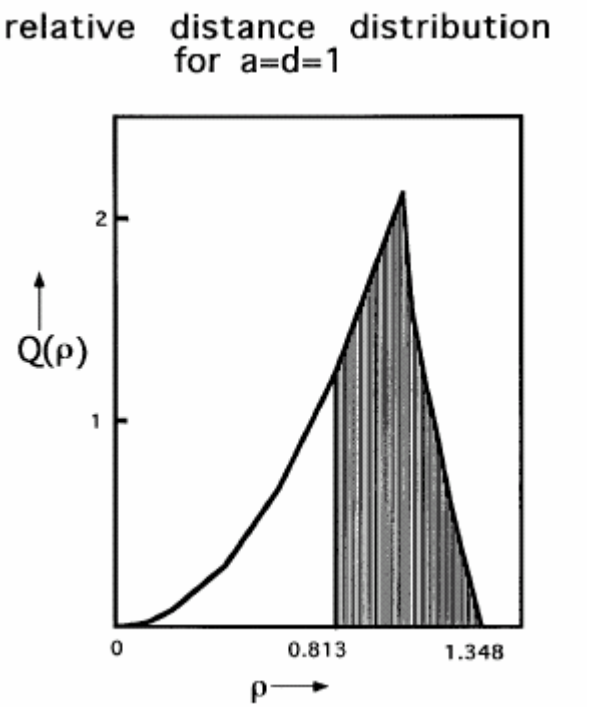

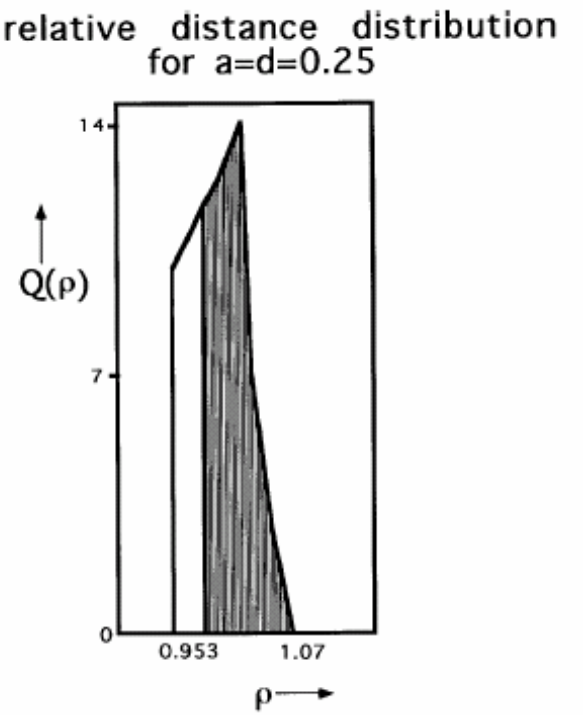

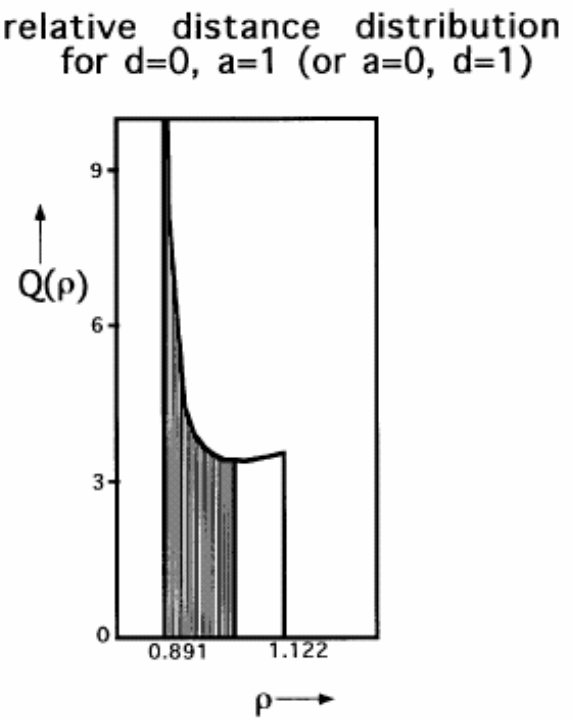

$\rho_{(max)}$: 1.070 (1.081) | $\rho_{(max)}$: 1.020 (1.027) | $\rho_{(max)}$: 0.891 (0.959)

B.W. van der Meer (2002) shaded area: 67% confidence interval with centre () ≠ $\rho_{(max)}$

the orientation factor κ^2 (15)

and the error on distance determination by FRET

party fixed transition dipole moments

one partly fixed + one free

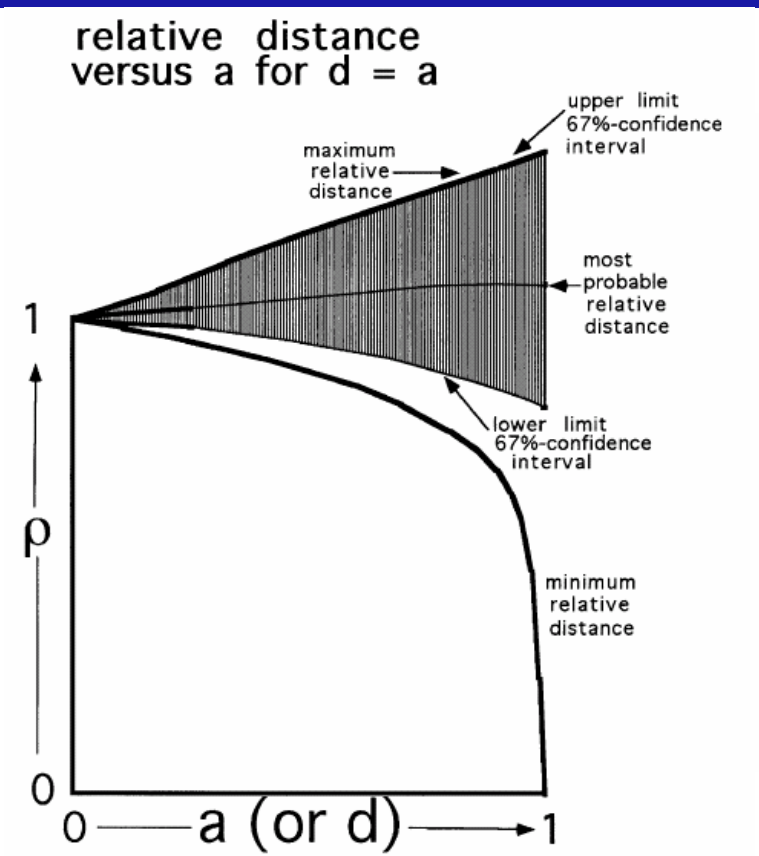

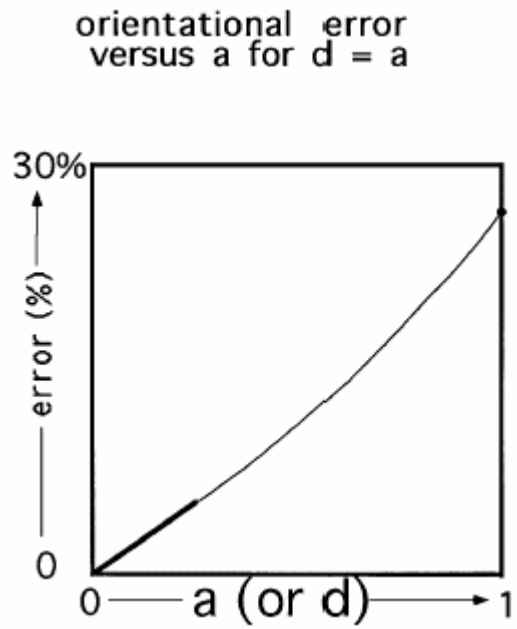

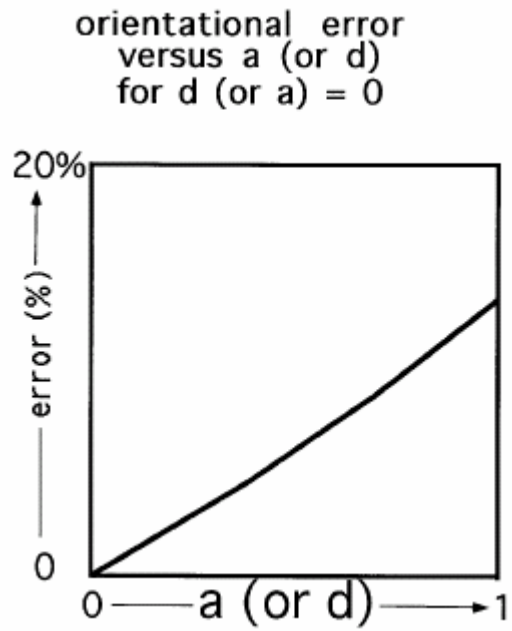

B.W. van der Meer (2002)

errors on distance determination

$$E_{FRET} = \frac{R_0^6}{R_0^6 + r^6}$$

$$R_0^6 = \frac{9000(\ln 10)\kappa^2 \varphi_D}{128\pi^5 n^4 N_A} J$$

three ε–subunit positions in F_0F_1-ATPsynthase during ATP synthesis:

L: r = 8.03 nm

M: r = 6.27 nm

H: r = 4.65 nm

error on H due to κ^2 ?

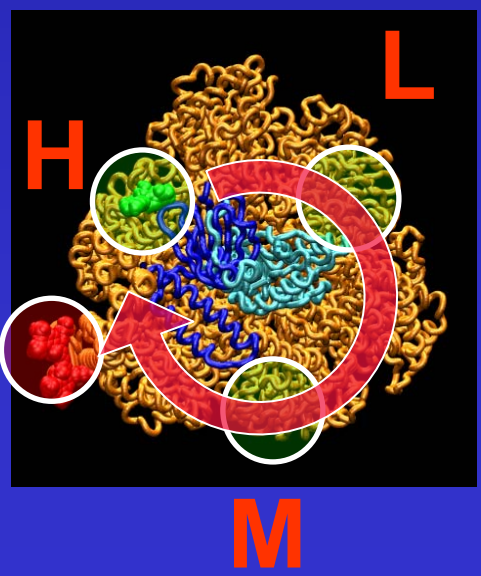

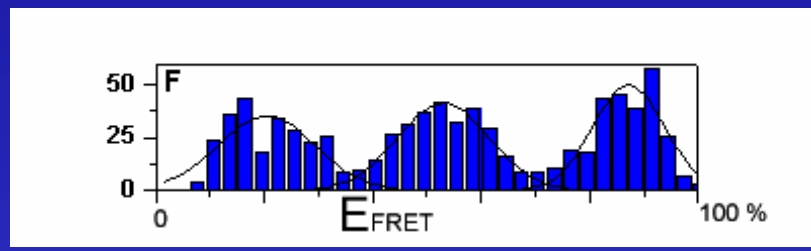

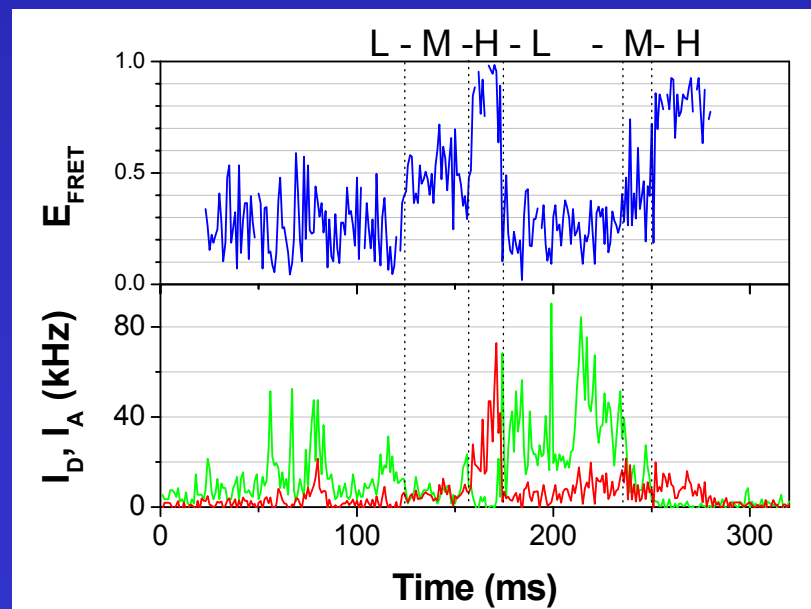

distance errors

three ε–subunit positions during ATP synthesis:

L: r = 8.03 nm

M: r = 6.27 nm

H: r = 4.65 nm

r_{0D} (TMR)= 0.06 → d=0.15

r_{0A} (Cy5)= 0.25 → a=0.65

$$\langle d_D \rangle = \langle d_D^x \rangle^2 = r_{0D} / 0.4$$

$$\langle d_A \rangle = \langle d_A^x \rangle^2 = r_{0A} / 0.4$$

error on H-state due to κ^2 is <10% !

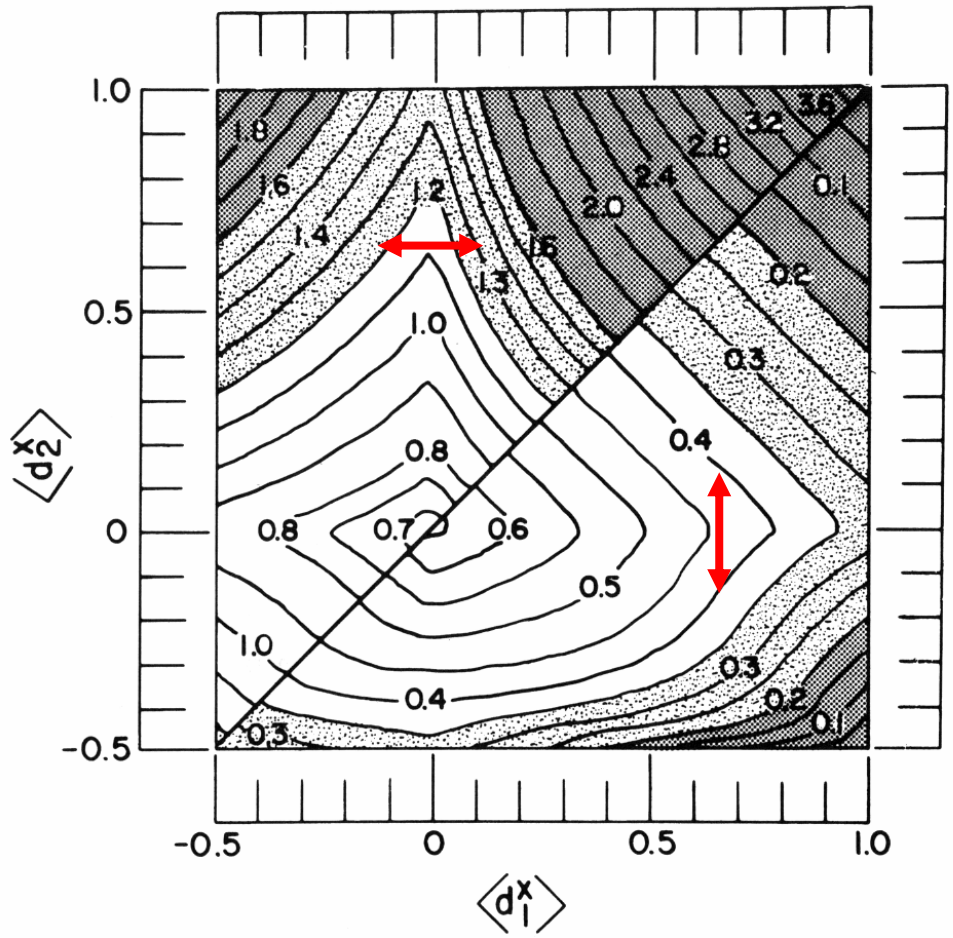

Figure 4.12. Contour plot for the case that d_T^X is not known. $\langle d_1^X \rangle$ represents $\langle d_D^X \rangle$ or $\langle d_A^X \rangle$, and $\langle d_2^X \rangle$ represents $\langle d_A^X \rangle$ or $\langle d_D^X \rangle$. The contours are symmetrical with respect to reflection on the diagonal. Therefore, both extrema can be shown in one plot, as is done here: Contours for the maximum $\langle \kappa^2 \rangle$ appear in the upper left half of the diagram, and those for the minimum in the lower left half. The maximum $\langle \kappa^2 \rangle$ is found at $\langle d_2^X \rangle$ = the largest of $\langle d_D^X \rangle$ and $\langle d_a^X \rangle$, and $\langle d_1^X \rangle$ is the smallest, whereas the minimum corresponds with the point where $\langle d_2^X \rangle$ = the smallest of $\langle d_D^X \rangle$ and $\langle d_A^X \rangle$, and $\langle d_1^X \rangle$ is the largest. Stippled regions of the contour plots indicate the uncertainty in the donor–acceptor separation, which results from using $\langle \kappa^2 \rangle = \frac{2}{3}$ instead of the appropriate minimum and maximum values for $\langle \kappa^2 \rangle$. The heavily stippled regions correspond to errors in this distance of more than 20%. The uncertainty is between 10% and 20% in the lightly stippled regions and less than 10% in the unstippled ones. (Reproduced from the *Biophysical Journal*, 1979, vol. 26, p. 175 [3] by copyright permission of the Biophysical Society.)

literature

- B. W. van der Meer, George Coker III, S.-Y. Simon Chen, Resonance Energy Transfer; VCH 1994
- B. W. van der Meer, Rev. Mol. Biotech. 82, 181-196 (2002).
- R. E. Dale, J. Eisinger. W. E. Blumberg, Biophys. J. 26, 161-194 (1979).

to be continued in October 2004.

- www.m-boersch.org slides
- email: m.boersch@physik.uni-stuttgart.de literature